CO ($J = 4 \rightarrow 3$) and 650 μm Continuum Observations of the z=0.93 Hyperluminous Infrared Galaxy FSC 15307+3252

M. S. Yun

National Radio Astronomy Observatory,[1] *P.O. Box 0, Socorro, NM 87801*

and

N. Z. Scoville

California Institute of Technology, Pasadena, CA 91125

ABSTRACT

We report the results of our CO $J = 4 \rightarrow 3$ line and rest frame 650 μm continuum observations of the z=0.93 hyperluminous infrared galaxy FSC 15307+3252 using the Owens Valley Millimeter Array. No line or continuum emission was detected, but the derived limits provide a useful constraint on the temperature, emissivity, and mass of the cold dust associated with FSC 15307+3252 and its molecular gas content.

The 3σ upper limit on the velocity integrated CO (4–3) line flux is 1.6 Jy km s^{-1} (for $\Delta V = 300$ km s^{-1}). This corresponds to a surprisingly small total molecular gas mass limit of $5 \times 10^9 h^{-2}\ M_\odot$ for this galaxy with infrared luminosity $L_{FIR} > 10^{13} L_\odot$. Combined with existing photometry data, our 3σ upper limit of 5.1 mJy for the 239 GHz (650 μm rest wavelength) continuum flux yields a total dust mass of 0.4-1.5 times $10^8\ M_\odot$. The CO luminosity (thus molecular gas content) and the resulting gas-to-dust ratio are lower than the values typical for the more gas-rich infrared galaxies, but they are within the observed ranges. On the other hand, FSC 15307+3252 has a dust content and infrared luminosity 40 and 200 times larger than the infrared bright elliptical-like galaxies NGC 1275 and Cygnus A.

The FIR luminosity to dust mass ratios, L_{FIR}/M_{dust}, for all three galaxies hosting a powerful AGN (FSC 10214+4724, FSC 15307+3252, Cygnus A) are larger than reasonably expected for a galaxy dominated by a starburst and four times larger than Arp 220. Therefore the bulk of the observe FIR luminosity in these galaxies is likely powered by their luminous active nucleus.

Subject headings: galaxies: individual (FSC 15307+3252) – galaxies: active – ISM: molecules – ISM: dust — galaxies: formation

[1]The National Radio Astronomy Observatory is a facility of the National Science Foundation operated under cooperative agreement by Associated Universities, Inc.

1. Introduction

The early evolution of galaxies may be extremely rapid with a burst of high luminosity. Optical searches for such ultraluminous proto-galaxies have been unsuccessful, indicating that such activity is obscured by dust extinction or by Lyman-continuum absorption (internal or intervening) and therefore not optically visible (e.g. Djorgovski et al. 1993). Alternatively, this may also mean that most galaxies do not have an early high luminosity phase. Millimeter wavelength CO and submillimeter dust continuum searches offer an alternative, extinction-free way of detecting high redshift proto-galaxies (see Yun & Scoville 1996, Evans et al. 1996, Smail et al. 1997, Hacking et al. 1997).

The first detection of CO emission from a cosmological distance was reported by Brown & Vanden Bout (1991) and by Solomon et al. (1992a) in the most distant infrared galaxy detected by the IRAS survey, FSC 10214+4724 at z=2.3 (Rowan-Robinson et al. 1991). The extended nature of the CO emission was later revealed by high resolution imaging (Scoville et al. 1995, Downes et al. 1997). In a unique study exploiting the magnifying property of gravitational lensing, the total gas mass and the detailed distribution of molecular gas in the z=2.6 quasar H 1413+117 were determined (Yun et al. 1997), and the derived gas properties are indeed remarkably similar to the IR luminous galaxies in the local universe ($d_{CO} \lesssim 1$ kpc, $n \geq 10^4$ cm^{-3}, $T_{ex} \geq$ 50-100 K). The compact and concentrated gas distribution suggests that the rapid metal enrichment of interstellar medium by a massive starburst may explain the strong CO emission. Redshifted CO emission has subsequently been detected in the z=4.7 quasar BR 1202−0725 (Ohta et al. 1996, Omont et al. 1996) and in the $z = 2.4$ radio galaxy 53W002 (Scoville et al. 1997a).

The hyperluminous infrared galaxy FSC 15307+3252 at $z_{opt} = 0.9257 \pm 0.0012$ is the second highest redshift object detected by IRAS and one of the most luminous galaxies known ($\nu L_{60\mu} = 4 \times 10^{12} L_{\odot}$, Cutri et al. 1994). Both the optical spectrum (Seyfert 2) and the radio continuum power ($\log P_{1.4GHz} = 25.1$ W Hz^{-1} – from the VLA FIRST Survey by Becker et al. 1995) suggest some nuclear activity, and the presence of polarized, broad optical emission lines suggests that this galaxy may host an obscured QSO (Hines et al. 1995, Liu et al. 1996). The observed properties of FSC 15307+3252, including the spectral energy distribution dominated by the infrared, are nearly identical to the more distant IRAS galaxy FSC 10214+4724, where bright (lensed) CO emission has already been detected. In general, strong dust emission is one of the best indicators of a large molecular gas content, and the large 60 μm luminosity and infrared-to-optical luminosity ratio suggest that FSC 15307+3252 is also a high redshift dusty, gas-rich galaxy. Therefore we have conducted a search for redshifted CO (4–3) emission and submillimeter continuum emission at $\lambda_{rest} = 650$ μm using the Owens Valley Millimeter Array between December 1996 and February 1997. Here we report the results of our search and the inferences on the dust and molecular gas content in this hyperluminous infrared galaxy.

2. Observations

FSC 15307+3252 was observed using the Owens Valley Millimeter Array in the low and equatorial configurations between December 1996 and February 1997. The array consists of six 10.4 m telescopes, and the longest baseline observed was 120 m. The redshifted CO (4–3) transition occurs at 239.41 GHz, and the primary beam of the 10.4-m telescope is 24.9″ (140 kpc at D_A = 1.16 Gpc[2]) at this frequency. The system temperatures were typically 600–900 K in the signal side-band corrected for antenna and atmospheric losses and for atmospheric incoherence. Spectral resolution was provided by a digital correlator configured with 120×4 MHz channels (5.0 km s^{-1}), covering a total velocity range of 600 km s^{-1}. The 239.4 GHz continuum emission was measured using a 1 GHz bandwidth analog correlator, and the 3mm continuum emission centered on 102.1 GHz was measured simultaneously using the 3mm SIS receivers (T_{sys} = 200–400 K). The total usable integration time on source was 19 hours distributed over 4 tracks in the two different telescope configurations. The nearby quasar 1611+343 (1.0 & 0.8 Jy at 102 & 239 GHz) was used to track the phase and gain variations. Neptune (T_b=90 K) and 3C 273 were observed for absolute flux calibration – see Table 1 for the observation summary. The data were calibrated using the standard Owens Valley array program mma (Scoville et al. 1992) and mapped using DIFMAP

[2] We adopt $H_\circ$ = 75 Mpc [km s^{-1}]$^{-1}$ and $q_\circ$ = 0.5 throughout this paper.

(Shepherd et al. 1994) and the NRAO AIPS package.

3. Results

3.1. CO (4–3) Emission

We searched for CO $J = 4 \rightarrow 3$ ($\nu_{rest} = 461.040811$ GHz) line emission in the redshift range z=0.9240-0.9275, but no CO emission was detected. The rms noise in each 80 MHz ($\Delta V = 100$ km s^{-1}) channel was 9 mJy beam^{-1} (see Figure 1). The derived upper limit on the molecular gas mass is $M_{H_2}(3\sigma) \leq 5.0 \times 10^9 h^{-2} M_\odot$, assuming a CO line width of 300 km s^{-1} and $M_{H_2}/L'_{CO} = 4\ M_\odot$ [K km s^{-1} pc^2]$^{-1}$. This is about 1/2 or 1/3 of the amount of molecular gas found in the ultraluminous infrared galaxies such as Arp 220 (see Sanders et al. 1991, Scoville et al. 1997b) and a factor two better than the upper limits reported by Evans et al. (1998) from their IRAM 30-m telescope observations. It is possible that the CO emission occurs at a redshift significantly different from the UV/optical emission line redshift we searched. However, the near-infrared spectroscopy of the narrow emission lines by Evans et al. (1998) confirms the redshift determined earlier by Cutri et al. (1994), and it is therefore likely that the CO emission in FSC 15307+3252 is intrinsically weak.

3.2. Continuum Emission

The continuum emission at 102 GHz and 239 GHz were measured simultaneously with the spectral line data using the analog continuum correlator with 1 GHz bandwidth. The rms noise estimated from the natural-weighted image was 0.43 mJy beam^{-1} at 102 GHz and 1.7 mJy beam^{-1} at 239 GHz. The spectral energy distribution (SED) of FSC 15307+3252 is shown in Figure 2 including the 3σ upper limits of 1.3 mJy and 5.1 mJy at λ_{rest} of 1500 μm and 650 μm and the photometric data from Cutri et al. (1994), Becker et al. (1995), and Aussel et al. (1998).

The spectral index between the IRAS measurement and our 650 μm upper limit, $\alpha(52\text{–}650\mu\text{m}) > 1.8$, is not large enough to rule out the possibility of a spectral break due to self-absorbed synchrotron emission. If the spectral break occurs at $\lambda \gtrsim 100$ μm, however, it would clearly exceed the theoretical limit ($\alpha = 2.5$) even if the 650 μm flux is close to the 3σ upper limit reported here, leaving thermal dust emission from a large amount of dust as the only reasonable explanation for the large FIR/submillimeter luminosity. The observed FIR and submillimeter SED can be described well by the thermal continuum emission from $T_{dust} = 50$ K dust with emissivity $\beta = 1.5$ (see below for a further discussion).

4. Discussion

4.1. Dust Temperature, Emissivity, and Mass

The flux density, S_ν, from a cloud at a distance D containing N spherical dust grains each of cross-section σ, temperature T, and emissivity $Q(\nu)$, is given by

$$S_\nu = N[\sigma/D^2]Q(\nu)B(\nu,T) \qquad (1)$$

The dust cloud mass can be obtained as the product of N, the assumed mean dust mass density ρ, and the mean volume of each dust particle v. The dust volume v can be related to the grain cross-section σ in Eq. 1, and the dust mass can be obtained from the observed flux as

$$M_{dust} = [S_\nu D^2/B(\nu,T)][(4/3)a/Q(\nu)]\rho \qquad (2)$$

where a is the grain radius (see Hildebrand 1983). The mass opacity coefficient $\kappa_\nu \equiv [(4/3)a\rho/Q(\nu)]^{-1}$ may be strongly dependent on frequency and dust composition, and its estimate and resulting dust mass are uncertain by a factor of at least three (see Hughes et al. 1993). Adopting $\kappa_\nu = 10$ g^{-1} cm^2 at $\lambda = 250\mu$m (Hildebrand 1983), Eq. 2 becomes

$$M_{dust} = 180 \frac{S_{250\mu m} D_L^2}{(1+z)} [exp(57.6/T_{dust}) - 1]\ M_\odot \qquad (3)$$

where $S_{250\mu m}$ is the 250 μm flux density in Jy and D_L is the luminosity distance in Mpc.

The continuum flux limits we obtained at millimeter and submillimeter wavelengths provide a useful constraint on the temperature, emissivity, and mass of the cold dust associated with FSC 15307+3252. For the gas rich infrared luminous galaxies such as Arp 220, the observed SED is consistent with the optical depth reaching unity near $\lambda \sim 100$ μm (Scoville et al. 1991, Solomon et al. 1997), and a high opacity at these wavelengths is also suggested by the faintness of 158 μm [C II] fine structure line emission observed in such galaxies (Malhotra et al. 1997, Fischer et al. 1998). We therefore model the observed FIR and submillimeter SED as the combination of a pure black-body spectrum at short wavelengths and a grey-body spectrum with emissivity β between 1 and 2 for the long wavelengths, with the transition occurring between 100 and 200 μm.

Three different "good" dust emission models for FSC 15307+3252 are listed in Table 2 and plotted in Figure 2. The IRAS 60 and 100 μm (λ_{rest} = 31 and 52 μm) data are well fit by a pure black-body spectrum ($\beta = 0$) with dust temperature of 85 K. At longer wavelengths, dust emission from 35 K dust with emissivity $\beta = 2.0$ (Model A) is consistent with the $\lambda_{rest} = 650$ μm upper limit and the 85 K black-body spectrum at shorter wavelengths. This also represents the maximum dust mass case ($M_{dust} = 1.5 \times 10^8 M_\odot$) among the variety of models considered because it has the lowest T_{dust} and predicts the largest 250 μm flux (see Eq. 3). Other $\beta = 2.0$ models with $T_{dust} \leq 30$ K and bound by the $\lambda_{rest} = 650$ μm upper limit do not connect smoothly with the 85 K black-body spectrum (IRAS data).

The actual observed spectra of luminous infrared galaxies such as Arp 220 and FSC 10214+4724 are well described by a dust model with emissivity $\beta \sim 1.5$ (see Table 3). A $\beta = 1.5$ model and $T_{dust} = 50$ K (Model B) is also consistent with the $\lambda_{rest} = 650$ μm upper limit and the 85 K black-body spectrum at shorter wavelengths. The derived dust mass is about 40% smaller than Model A mainly due to higher dust temperature.

Given the limited data available, an exhaustive search for the best model is not warranted, and the "good" dust models shown here are not unique. Nevertheless some meaningful limits on the dust temperature and emissivity can be set by the observations. For example, a dust spectrum with $T_{dust} = 50$ K and emissivity $\beta = 1.0$ produces too much 650 μm emission when connected smoothly with the black-body spectrum at shorter wavelengths. Similarly, model spectra with $T_{dust} = 40$ K and $\beta \leq 1.5$ are excluded by the data. Using these constraints, a minimum dust mass model with the highest T_{dust} allowed by the IRAS data points and the largest β physically meaningful may be constructed and is shown as Model C in Table 2 and Figure 2. The minimum dust mass for FSC 15307+3252 (Model C) is 3.5×10^7 $M_\odot$, which is about 1/4 of the maximum dust mass in Model A.

In summary, a wide range of possible dust models considered here have produced a relatively narrow range of total dust mass for FSC 15307+3252. A few clarifying remarks should made here, however. First of all, our modeling offers a robust estimate for the *total* dust mass as the cold dust component in the submillimeter band dominates the total dust mass. This is clearly demonstrated by the fact that the apparent difference in the observed flux density between the 85 K and 200 K dust component is only a factor of three near $\nu_{rest} = 10^{12.8}$ Hz (see Figure 2) but the warmer component accounts for only about 1% in dust mass because of strong temperature dependence on flux density. Secondly, while it is conceivable that a much larger quantity of extremely cold dust may be present in this galaxy for the same reason, the dust models listed in Table 2 are nevertheless the most relevant in understanding the nature of FSC 15307+3252. In theory, there could be an arbitrarily large amount of dust at or near the cosmic background temperature ($T_{CMB} = 5.3$ K) because such a dust component would not contribute much to the observed SED. On the other hand, such cold dust, if present, would not be found in the area of the galaxy associated with the strong heating, and it would be irrelevant to the physics of energetic processes observed in this galaxy. Therefore the relevant maximum total dust mass for FSC 15307+3252 is about $1.5 \times 10^8 M_\odot$.

4.2. Comparison with Ultraluminous Infrared Galaxies

The extremely dusty nature of FSC 15307+3252 is easily seen when it is compared to the two well studied infrared luminous galaxies FSC 10214+4724 and Arp 220. As summarized in Table 3, the FIR luminosity of FSC 15307+3252 is 10 times larger than Arp 220 while their optical B band luminosities are comparable. The L_{FIR}/L_B ratio of 650 is about four times larger than both FSC 10214+4724 and Arp 220, and the dominance of the FIR in its bolometric luminosity is the most extreme among all known objects.

For optically thick black-body emission (at $\lambda \lesssim 100$ μm) originating from a single source with a radius R, the source size can be determined as $R = [\frac{S_\nu D_L^2}{\pi B(\nu,T)}]^{1/2}$ – for a distributed source, this radius corresponds to $(A/\pi)^{1/2}$ where A is the effective area of the optically thick clouds. For FSC 15307+3252 at D_L = 4.3 Gpc and S_ν = 510 mJy in the IRAS 100 μm band, the black body radius is 370 pc for T_{dust} = 85 K. In Arp 220, the 100 μm black body radius is 180 pc, which is comparable to the size of the nuclear molecular gas complex (R_{CO} = 230 pc – Scoville et al. 1997b). The size of the CO emitting region inferred from the gravitational lensing model for the Cloverleaf Quasar at $z = 2.6$ (H 1413+117; Yun et al. 1997) is also similar.

Both Arp 220 and FSC 10214+4724 are gas rich systems with molecular gas contents in excess of 10^{10} $M_\odot$ and gas-to-dust ratios of 260 & 500, respectively. These ratios are typical of luminous infrared galaxies in the IRAS Bright Galaxy Sample ($M_{H_2}/M_{dust} = 540 \pm 290$; Sanders et al. 1991). However, given its large infrared luminosity it is surprising that no CO emission is detected in FSC 15307+3252 by our observations. The 3σ upper limit on its CO luminosity implies an upper limit on molecular gas mass of $M_{H_2}(3\sigma) \leq 8.8 \times 10^9 M_\odot$, which is less than the typical molecular gas content in infrared luminous galaxies like Arp 220 even though its FIR luminosity is nearly 10 times larger. The well known relationship between the FIR and CO luminosity (see review by Young & Scoville 1991) has a second order trend of increasing L_{FIR}/L_{CO} [equivalently, L_{FIR}/M_{H_2}] ratio with increasing infrared luminosity. The observed large L_{FIR}/L_{CO} ratio in FSC 15307+3252 is generally consistent with this trend, but the observed CO luminosity is still at least 10 times too small compared to the predicted relation. Therefore, the FIR emission in FSC 15307+3252 has a clear and large excess over the mechanisms operating in other infrared luminous galaxies such as Arp 220.

A possible explanation for the enhanced FIR luminosity and apparent large L_{FIR}/M_{H_2} ratio (> 1500) is that the mean dust temperature is globally higher in FSC 15307+3252 compared to other infrared luminous galaxies. The dust models most consistent with the SED for FSC 15307+3252 have dust temperatures 10 to 20 K warmer than in Arp 220 ($T_{dust} = 42$ K, $\beta = 1.3$ for $\lambda \geq 100$ μm and $T_{dust} = 65$ K for $\lambda \leq 100$ μm – Scoville et al. 1991). The flux density (or luminosity) has an exponential dependence on dust temperature (see Eq. 3), and a relatively small increase in mean dust temperature can dramatically increase the observed FIR luminosity even without any increase in the total dust mass. The inferred gas-to-dust ratio of $\leq$ 60-250 from the dust model (§4.1) is somewhat low but still consistent with the ratios seen in other galaxies.

4.3. Comparison with Infrared Bright Elliptical-like Galaxies

While Arp 220 and other ultraluminous infrared galaxies in the local universe are typically ongoing mergers of two gas rich spiral galaxies (see Hibbard & Yun 1998), FSC 15307+3252 appears to be a giant elliptical galaxy, with possible companions (Soifer et al. 1994, Evans et al. 1998). While the observed gas and dust properties of FSC 15307+3252 are consistent with those of infrared luminous galaxies, the absence of bright CO emission (and resulting extreme L_{FIR}/M_{H_2} ratio) and the presence of a buried luminous AGN (Hines et al. 1995, Liu et al. 1996) warrant comparisons with other types of objects. In particular, we compare the observed properties of FSC 15307+3252 with other infrared bright giant elliptical-like galaxies hosting a luminous AGN.

The giant central galaxy of the Perseus cluster, NGC 1275 (Perseus A, 3C 84), offers an interesting comparison as it is a well known infrared source whose cold gas content is also well documented ($M_{H_2} = 6 \times 10^9$ $M_\odot$; Lazareff et al. 1989, Mirabel et al. 1989, Jaffe 1990, Reuter et al. 1993, Inoue et al. 1996). We have constructed the SED for this galaxy from the literature and the OVRO and VLA archival flux databases (the central radio source was in its quiescent phase during the winter observing season of 1997-1998). Its cold dust content is estimated by subtracting a smooth polynomial component (non-thermal contribution from the AGN) from the observed FIR SED. As summarized in Table 3, the observed submillimeter-FIR SED can be modeled as dust emission arising from relatively cool dust ($T_{dust} \sim 40$ K) with a total mass of about 2×10^6 $M_\odot$. The optical luminosity of the underlying galaxy is nearly identical to that of FSC 15307+3252, but both the total FIR luminosity and the dust mass are considerably lower (by factors of 260 and 40, respectively). High resolution studies of molecular gas and FIR emission have shown that the associated star forming activity occurs spread over a 10 kpc area in NGC 1275 (Reuter et al. 1993, Inoue et al. 1996, Lester et al. 1995), and this explains the low L_{FIR}/M_{H_2} ratio (8.3) and low dust temperature. Part of the observed infrared emission may also arise in the foreground system currently colliding onto NGC 1275 (see Minkowski 1957, Caulet et al. 1992).

The radio galaxy Cygnus A offers another interesting comparison since it is a giant elliptical galaxy hosting a buried quasar nucleus (Djorgovski et al. 1993, Ogle et al. 1997). The optical luminosity of the host galaxy in Cygnus A is about 3 times fainter than FSC 15307+3252, but most of its total luminosity emerges in the infrared ($L_{FIR}/L_B = 30$) as in

FSC 15307+3252. The SED of Cygnus A, excluding the contribution from the radio lobes, is shown in Figure 3, and the observed submillimeter-FIR SED can be modeled as thermal emission arising from about 2×10^6 $M_\odot$ of dust with $T_{dust} \sim 50$ K. Again, both the FIR luminosity and total dust mass are considerably less than those of FSC 15307+3252 (by factors of 76 and 40, respectively). Previous CO observations have reported only upper limits for the molecular gas mass ($\sim 10^{10} M_\odot$, Mirabel et al. 1989, Mazzarella et al. 1993, McNamara & Jaffe 1994). Given its low dust mass, at least an order of magnitude improvement in sensitivity will be needed to detect the CO emission.

4.4. Starburst versus AGN

In ultraluminous infrared galaxies, the highly luminous activity originating from the central region less than 1 kpc in size is opaque even at FIR wavelengths ($A_V \geq 10^3$), and a hotly debated issue is whether the hidden source of luminosity is a massive starburst or an AGN. There is little doubt that young massive stars are forming within the massive central gas complexes in all cases, and evidence for an AGN, such as broad emission lines or excess radio emission, is present in some of the luminous infrared galaxies. The difficult unresolved issue, however, is whether a starburst or an AGN is the dominant source of the observed luminosity.

For the luminous infrared galaxies where the majority of the bolometric luminosity emerges in the infrared, the ratio of infrared luminosity to total gas mass (L_{FIR}/M_{H_2}) is a measure of efficiency of converting gas mass into luminosity (Scoville et al. 1991, Sanders et al. 1991). For a starburst population with a reasonable IMF, the ratio L/M_{dyn} should be less than 500 $L_\odot/M_\odot$ (Leitherer & Heckman 1995, Scoville et al. 1997b), and objects with an L_{FIR}/M_{H_2} ratio > 500 $L_\odot/M_\odot$ require a significant luminosity contribution from an active nucleus.

Among the galaxies discussed above, only upper limits on the gas mass exist for FSC 15307+3252 and Cygnus A. However, the ratio L_{FIR}/M_{dust} can still be examined. As shown in Table 3, this ratio for FSC 10214+4724, FSC 15307+3252, and Cygnus A is 4 to 15 times larger than for Arp 220, and the inferred L_{FIR}/M_{H_2} ratio approaches 500 $L_\odot/M_\odot$ (assuming a reasonable gas-to-dust ratio of ~ 200), which is difficult to explain with a starburst alone. This result is perhaps not surprising as all three sources probably host a quasar-like luminous AGN. In NGC 1275, the L_{FIR}/M_{dust} ratio is similar to that of Arp 220, but the situation is not clear because the bulk of the gas and dust may lie well outside the influence of the AGN.

4.5. Other Dusty High Redshift Galaxies

Lastly, it is worth noting that there is a growing list of high redshift galaxies with a clear submillimeter dust continuum detection but without correspondingly bright CO emission. This list includes the z=4.3 radio galaxy 8C 1435+635 (Ivison 1995, Ivison et al. 1998), the z=3.8 radio galaxy 4C 41.17 (Chini & Krügel 1994, Dunlop et al. 1994, Yun & Scoville 1996), and the z=2.8 radio galaxy MG 1019+0535 (Yun & Scoville 1996, Cimatti et al. 1998) – also see the review by Evans (1997). Inferred dust masses of about 10^8 $M_\odot$ are reported for these systems, but their dust masses are nearly unconstrained because their dust continuum detections in most cases are limited to just one or two data points near the peak of their dust spectrum ($\lambda_{rest} \sim 200$ μm). Existing CO observations of these systems place rather large gas mass limits of about 10^{11} $M_\odot$ (Yun & Scoville 1996, Evans et al. 1996, van Ojik et al. 1997, Ivison et al. 1998) – comparable to the most gas-rich galaxies in the local universe but probably not sufficient to detect the gas associated with the dust observed at submillimeter wavelengths. These observations are still consistent with the formation of luminous galaxies in the early epochs. More sensitive CO observations are needed for a better comparison of their gas and dust properties.

5. Summary and Concluding Remarks

We report the results of CO (4–3) line and rest frame 650 μm continuum observations of the z=0.93 hyperluminous infrared galaxy FSC 15307+3252. No CO emission was detected within the redshift range of z=0.9240-0.9275, and we place an upper limit on the molecular gas mass of $\leq 5.0 \times 10^9 h^{-2} M_\odot$ for this galaxy with $L_{FIR} > 10^{13}$ $L_\odot$. We have also obtained a 3σ upper limit on the rest frame 650 μm continuum flux of 5.1 mJy. Combined with existing data, an SED which is completely dominated by the emission in the FIR emerges ($L_{FIR}/L_B = 650$). Several dust models consistent with the data can be constructed, and they all imply a total dust mass associated with the bright FIR emission in FSC 15307+3252 of 0.4-1.5 times 10^8 $M_\odot$.

The gas and dust properties of FSC 15307+3252 are compared with those of the luminous infrared galaxies FSC 10214+4724 and Arp 220. The CO luminosity (molecular gas content) and gas-to-dust ratio are somewhat low ($M_{gas}/M_{dust} \leq$ 60-250) but are within the range of observed properties for more gas-rich infrared galaxies. FSC 15307+3252 does not compare well with two infrared bright elliptical-like galaxies NGC 1275 and Cygnus A because its FIR luminosity and dust content are 100 and 40 times larger, respectively.

In conclusion, the observed gas and dust properties of the z=0.93 hyperluminous infrared galaxy FSC 15307+3252 are consistent with those of a massive galaxy with a large amount of dust (and possibly gas). The high dust temperature and large L_{FIR}/M_{dust} ratio ($\geq 10^5$) suggest that a large fraction of the luminosity may come from the luminous central AGN.

The authors are grateful to A. Evans, T. Phillips, and M. Gerin for helpful discussions and thank B. Butler for carefully reading this manuscript. The Owens Valley millimeter array is supported by NSF grants AST 93-14079 and AST 96-13717. M. Yun is supported by an NRAO Jansky Fellowship. This research has made use of the NASA/IPAC Extragalactic Database (NED) which is operated by the Jet Propulsion Laboratory, California Institute of Technology, under contract with the National Aeronautics and Space Administration.

Note added to the proof: After this manuscript was accepted for press, we learned about the new ISO far-infrared observations of 10 quasars and radio galaxies by Haas et al. (1998). The dust mass derived for Cygnus A by Haas et al. is in good agreement with our estimate given in Table 3.

REFERENCES

Aussel, H., Gerin, M., Boulanger, F., Désert, F.X., Casoli, F., Cutri, R.M., & Signore, M 1998, A&A, 334, L73

Becker, R.H., White, R.L., & Helfand, D.J. 1995, ApJ, 450, 559

Brown, R., & Vanden Bout, P. 1991, AJ, 102, 1956

Caulet, A., Woodgate, B. E., Brown, L. W., Gull, T. R., Hintzen, P. et al. 1992, ApJ, 388, 301

Chini, R., & Krügel, E. 1994, A&A, 288, L33

Cimatti, A., Freudling, W., Röttgering, H. J. A., Ivison, R. J., & Mazzei, P. 1998, A&A, 329, 399

Cutri, R.M., Huchra, J.P., Low, F.J., Brown, R.L., Vanden Bout, P.A. 1994, ApJ, 424, 65

Djorgovski, S., Weir, N., Matthews, K., & Graham, J. R. 1991, ApJ, 372, L67

Djorgovski, S., & Thompson, D. 1993, in *IAU Symp. 149, The Stellar Populations in Galaxies*, eds. Renzini, A., Barbuy, B. (Kluwer, Dordrecht), p337

Downes et al. 1997, in *Highly Redshifted Radio Lines*, eds. C. Carilli, S. Radford, K. Menten, & G. Langston, in press.

Dunlop, J. S., Hughes, D. H., Rawlings, S., Eales, S. A., & Ward, M. J. 1994, Nature, 370, 347

Evans, A. S., in *Highly Redshifted Radio Lines*, eds. C. Carilli, S. Radford, K. Menten, & G. Langston, in press.

Evans, A. S., Sanders, D. B., Mazzarella, J. M., Solomon, P. M., Downes, D., Kramer, C., & Radford, S. J. E., 1996, ApJ, 457, 658

Evans, A. S., Sanders, D. B., Cutri, R. M., Radford, S. J. E., Surace, J. A. et al. 1998, ApJ, in press.

Fich, M., & Hodge, P. 1991, ApJ, 374, L17

Fischer et al. 1998, in *Extragalactic Astronomy in the Infrared*, eds. G.A. Mamon, T.X. Thuan, & J.T.T. Van, (Editions Frontieres, Gif-sur-Yvette), in press.

Haas, M., Chini, R., Meisenheimer, K., Stickel, M., Lemke, D., Klaas, U., & Kreysa, E. 1998, ApJ, in press.

Hacking, P., Gautier, T. N., Herter, T. L., Lonsdale, C. J., Shupe, D. L. et al. 1997, in *Extragalactic Astronomy in the Infrared*, eds. G. A. Mamon, T. X. Thuan, J. Tran Thanh Van (Editions Frontieres)

Helou, G., Khan, I. R., Malek, L., & Boehmer, L. 1988, ApJS, 68, 151

Hibbard, J. E., & Yun, M. S. 1998, in preparation

Hildebrand, R.H. 1983, QJRAS, 24, 267

Hines, D.C., Schmidt, G.D., Smith, P.S., Cutri, R.M., Low, F.J. 1995, ApJ, 450, 1

Hughes, D. H., Robson, E. I., Dunlop, J. S., & Gear, W. K. 1993, MNRAS, 263, 607

Inoue, M. Y., Kameno, S., Kawabe, R., Inoue, M., Hasegawa, T., & Tanaka, M. 1996, AJ, 111, 1852

Ivison, R. J. 1995, MNRAS, 275, L33

Ivison, R. J., Dunlop, J. S., Hughes, D. H., Archibald, E. N., Stevens, J. A., Holland, W. S., Robson, E. I., Eales, S. A., Rawlings, S., Dey, A., & Gear, W. K. 1998, ApJ, 494, 211

Jaffe, W. 1990, A&A, 240, 254

Krügel, E., Steppe, H., & Chini, R. 1990, A&A, 299, 17

Lazareff, B., Castets, A., Kim, D.-W., & Jura, M. 1989, ApJ, 336, L13

Leitherer, C., & Heckman, T. M. 1995, ApJS, 96, 9

Lester, D. F., Zink, E. C., Doppmann, G. W., Gaffney, N. I., Harvey, P. M., Smith, B. J., & Malkan, M. 1995, ApJ, 439, 185

Liu, M.C., Graham, J.R., Wright, G.S. 1996, ApJ, 470, 771

Malhotra et al. 1997, ApJ, 419, L27

Mazzarella, J.M., Graham, J.R., Sanders, D.B., & Djorgovski, S. 1993, ApJ, 409, 170

McNamara, B.R., & Jaffe, W. 1994, A&A, 281, 673

Minkowski, in IAU Symp. 4, *Radio Astronomy*, ed. H. C. van de Hulst (Cambridge: Cambridge University Press), p107

Mirabel, I. F., Sanders, D. B., & Kazes, I. 1989, ApJ, 340, L9

Ogle, P. M., Cohen, M. H., Miller, J. S., Tran, H. D., Fosbury, R. A. E., & Goodrich, R. W. 1997, ApJ, L37

Ohta, K., Yamada, T., Nakanishi, K., Kohno, K., Akiyama, M. & Kawabe, R. 1996, Nature, 382, 426

Omont, A., Petitjean, P., Guilloteau, S., McMahon, R. G. & Solomon, P. M. 1996, Nature, 382, 428

Reuter, H.-P., Pohl, M., Lesch, H., & Sievers, A.W. 1993, A&A, 277, 21

Robson, E. I., & Leeuw, L. 1997, BAAS, 191, 22.01

Rowan-Robinson, M. Broadhurst, T., Lawrence, A., McMahon, R.G., Lonsdale, C.J., Oliver, S.J., Taylor, A.N., Hacking, P.B., Conrow, T., Saunders, W., Ellis, R.S., Efstathiou, G.P., Condon, J.J. 1991, Nature, 351, 719

Sanders, D. B., Scoville, N.Z., & Soifer, B. T. 1991, ApJ, 370, 158

Scoville, N. Z., Sargent, A. I, Sanders, D. B., & Soifer, B. T. 1991, ApJ, 366, L5

Scoville, N. Z., Carlstrom, J. C., Chandler, C. J., Phillips, J. A., Scott, S. L., Tilanus, R. P., & Wang, Z. 1992, PASP, 105, 1482

Scoville, N. Z., Yun, M. S., Brown, R. L. & Vanden-Bout, P. A. 1995, ApJ, 449, L109

Scoville, N.Z., Yun, M.S., Windhorst, R.A., Keel, W.C., Armus, L. 1997a, ApJ, 485, L21

Scoville, N. Z., Yun, M. S. & Bryant, P. 1997b, ApJ, 484, 702

Shepherd, M. C., Pearson, T. J., & Taylor, G. B. 1994, BAAS, 26, 987

Smail, I. Ivison, R. J., & Blain, A. W. 1997, ApJ, 490, L5

Soifer, B. T., Neugebauer, G., Matthews, K., & Armus, L. 1994, ApJ, 433, L69

Solomon, P. M., Downes, D., & Radford, S. J. E. 1992a, Nature, 356, 318

Solomon, P. M., Downes, D., & Radford, S. J. E. 1992b, ApJ, 398, L29

Solomon, P.M., Downes, D., Radford, S.J.E., Barrett, J.W. 1997, ApJ, 478, 144

Telesco, C.M. 1993, MNRAS, 263, L37

van Ojik, R., Röttgering, H. J. A., van der Werf, P. P., Miley, G. K., Carilli, C. L., Visser, A., Isaak, K. G., Lacy, M., Jenness, T., Sleath, J., & Wink, J. 1997, A&A, 321, 389

Young, J. S. & Scoville, N. Z. 1991, ARAA, 29, 581

Yun, M. S., & Scoville, N. Z. 1996, in *IAU Symposium 170, CO: 25 Years of Millimeter Spectroscopy*, eds. W. B. Latter, S. J. E. Radford, P. R. Jewell, J. G. Mangum, & J. Bally (Kluwer: Dordrecht), p341

Yun, M. S., Scoville, N. Z., Carrasco, J. J., & Blandford, R. D. 1997, ApJ, 479, L9

This 2-column preprint was prepared with the AAS LaTeX macros v4.0.

Fig. 1.— Average spectrum of CO (4–3) emission in FSC 15307+3252 smoothed to 80 MHz ($\Delta V = 100$ km s^{-1}) resolution (sampled at every 40 MHz) is shown for a $3''$ aperture centered on the position of FSC 15307+3252. The rms noise in each 80 MHz (100 km s^{-1}) channel map is 9 mJy beam^{-1}. The inferred 3σ upper limit on total molecular gas mass is $5.0 \times 10^9 h^{-2}\ M_\odot$.

Fig. 2.— Spectral Energy Distribution of FSC 15307+3252. Three "good" models for dust emission summarized in Table 2 are shown along with the 200 K black body spectrum appropriate for mid- and near-infrared features. The total dust mass inferred from the maximum (Models A) and the minimum (Model C) mass models lies between 0.4 and 1.5 times $10^8\ M_\odot$. The continuum data points for FSC 15307+3252 come from Cutri et al. (1994), Becker et al. (1995), Aussel et al. (1998) and this work. The filled squares represent detections and the filled triangles represent 3σ upper limits. The near-infrared photometric data from the ISO observations (filled diamonds) are interpreted as the emission from hot dust ($T \sim 400$ K), subtending less than 10 pc in total area (Aussel et al. 1998).

Fig. 3.— Comparison of spectral energy distributions in infrared luminous galaxies and dusty giant elliptical galaxies. The data for FSC 10214+4724, NGC 1275, and Cygnus A are scaled for an easier comparison. The dotted curves correspond to the dust models described in Table 3. Photometry data are assembled from the literature and the NASA/IPAC Extragalactic Database (NED). References include: FSC 10214+4724 (Rowan-Robinson et al. 1991, Telesco 1983); FSC 15307+3252 (this work, Cutri et al. 1994, Becker et al. 1995); Arp 220 (Scoville et al. 1991, 1997b); NGC 1275 (Fich & Hodge 1991, Lester et al. 1995); Cygnus A (Djorgovski et al. 1993, Robson & Leeuw 1997). As in Figure 2, upside-down triangles represent 3σ upper limits.

Table 1
Summary of CO Observations and the Derived Properties

RA (B1950)	$15^h30^m44^s.6$
DEC (B1950)	$+32°52'51''.0$
z_{CO} searched	0.9240-0.9275
Luminosity Distance[a]	4.33 Gpc
Angular-Size Distance[a]	1.16 Gpc $(1'' \rightarrow 5.6$ kpc)
θ (FWHM)	$2''.8 \times 3''.8$
$S_{102GHz}(3\sigma)$	≤ 1.3 mJy
$S_{239GHz}(3\sigma)$	≤ 5.1 mJy
$S_{CO}\Delta V(3\sigma)$[b]	≤ 1.6 Jy km s^{-1}
$L'_{CO}(3\sigma)$[b]	$\leq 2.2 \times 10^9$ K km s^{-1}pc^2
$M_{H_2}(3\sigma)$[c]	$\leq 8.8 \times 10^9$ M$_\odot$

[a]$H_o = 75$ km s^{-1} Mpc^{-1}, $q_o = 0.5$

[b]assuming $\Delta V = 300$ km s^{-1}

[c]using a standard conversion α=4 M$_\odot$ (K km s^{-1} pc^2)$^{-1}$

Table 2
Dust Models for FSC 15307+3252

Model	T_{dust}	$\beta^\dagger$	M_{dust}
Model A	35 K	2.0	1.5×10^8 $M_\odot$
Model B	50 K	1.5	9.2×10^7 $M_\odot$
Model C	65 K	1.5	3.5×10^7 $M_\odot$

$^\dagger\beta$ is emissivity index, i.e. $Q(\nu) \propto \nu^\beta$ (see Eq. 1).

Table 3

Comparison of Infrared Bright Galaxies

	F10214+4724[a]	F15307+3252	Arp 220	NGC 1275	Cygnus A
D_L^b (Mpc)	11800	4330	77	72	224
log L_B ($L_\odot$)[b]	12.10	10.31	10.05	10.53	9.78
log L_{FIR} ($L_\odot$)[c]	14.27	13.12	12.12	10.70	11.24
log M_{H_2} ($M_\odot$)[d]	11.34	<9.95	10.28	9.78	<9.54
T_{dust} (K)[e], β	75, 1.3	50, 1.5	42, 1.3	40, 1.5	50, 1.5
log M_{dust} ($M_\odot$)[f]	8.64	7.54-8.18	7.87	6.25	6.35
L_{FIR}/L_B	150	650	120	1.5	30
L_{FIR}/M_{H_2}	850	>1500	70	8.3	>50
M_{H_2}/M_{dust}	500	<60-250	260	3400	<1500
L_{FIR}/M_{dust}	4.3×10^5	0.9-3.8$\times 10^5$	1.8×10^4	2.8×10^4	7.8×10^4

[a]magnification due to gravitational lensing not included.

[b]log $L_B = 11.898 - 0.4m_B + 2 \log D_L$, where D_L is the luminosity distance in Mpc assuming $H_o = 75$ km s^{-1} Mpc^{-1}, $q_o = 0.5$

[c]computed from IRAS 60 & 100 μm fluxes for Arp 220, NGC 1275, & Cygnus A (see Helou et al. 1988) and computed from the adopted dust model SEDs for FSC 10214+4724 and FSC 15307+3252.

[d]using α=4 M$_\odot$ (K km s^{-1} pc^2)$^{-1}$

[e]derived from the dust models shown in Figure 3.

[f]see Eq. 3.

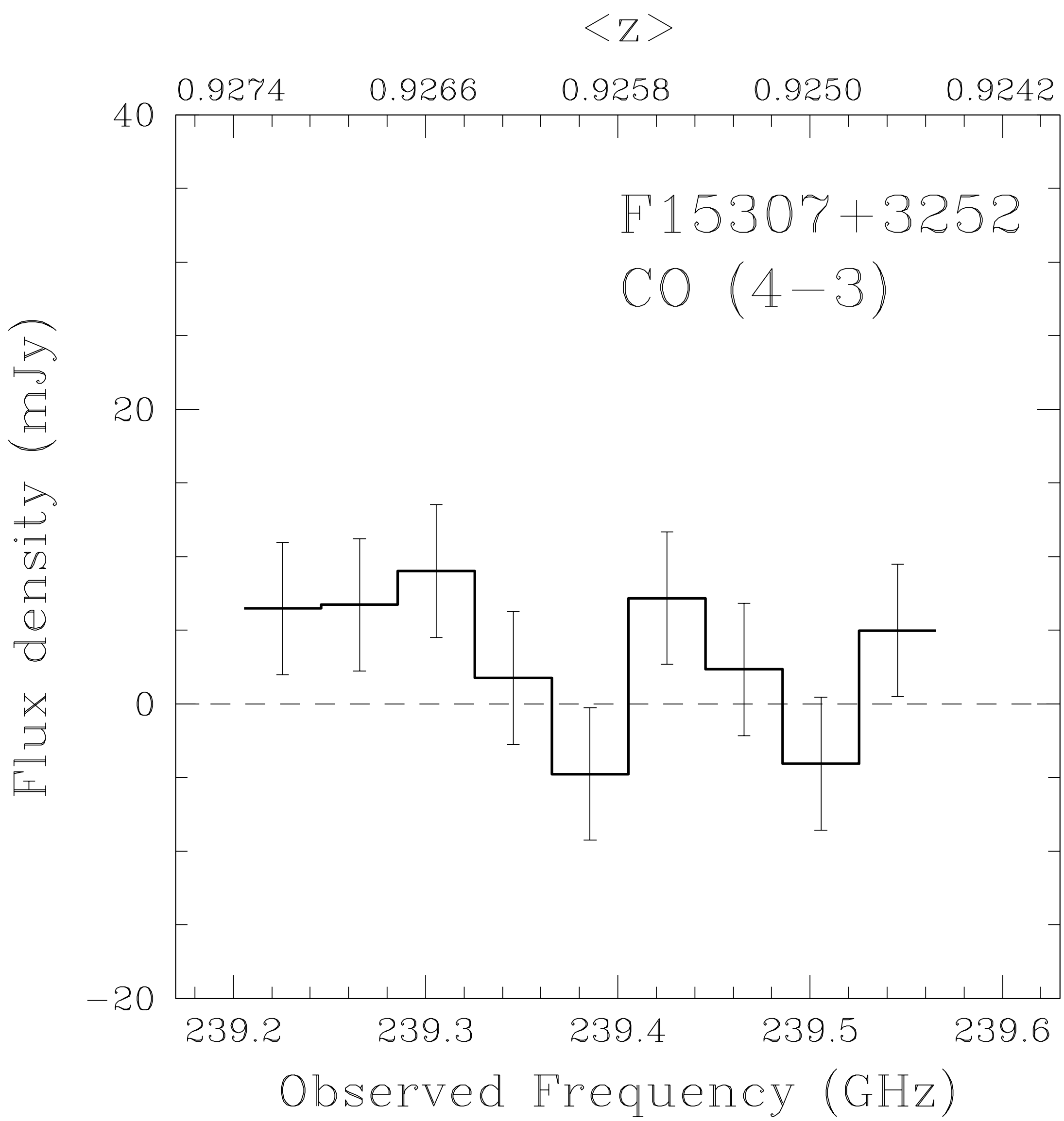

<z>
0.9274
0.9266
0.9258
0.9250
0.9242
40
20
0
−20
F15307+3252
CO (4−3)
Flux density (mJy)
239.2
239.3
239.4
239.5
239.6
Observed Frequency (GHz)

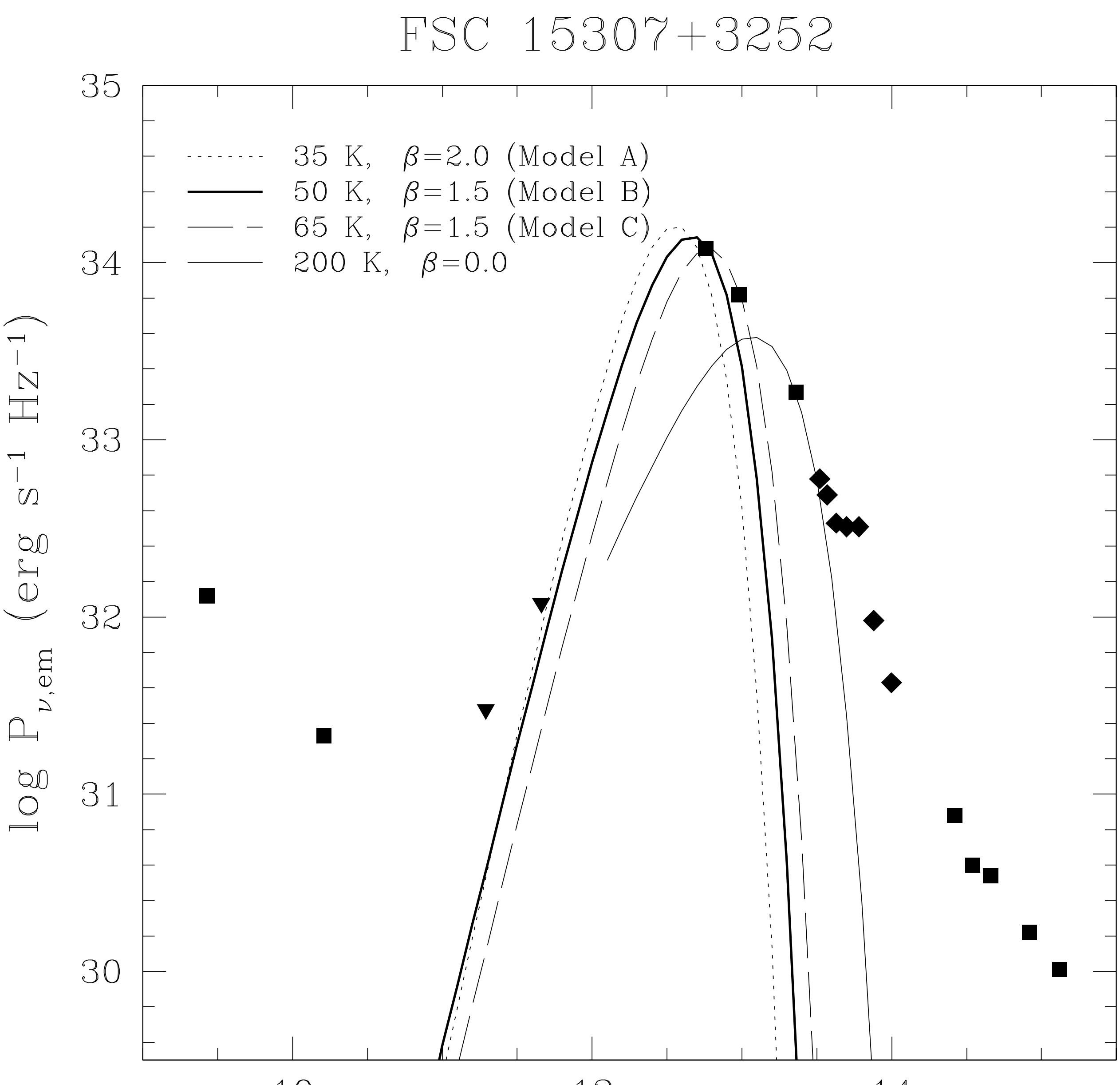

FSC 15307+3252
35 K, β=2.0 (Model A)
50 K, β=1.5 (Model B)
65 K, β=1.5 (Model C)
200 K, β=0.0
log P ν,em (erg s−1 Hz−1)
log Rest Frequency (Hz)
35
34
33
32
31
30
10
12
14

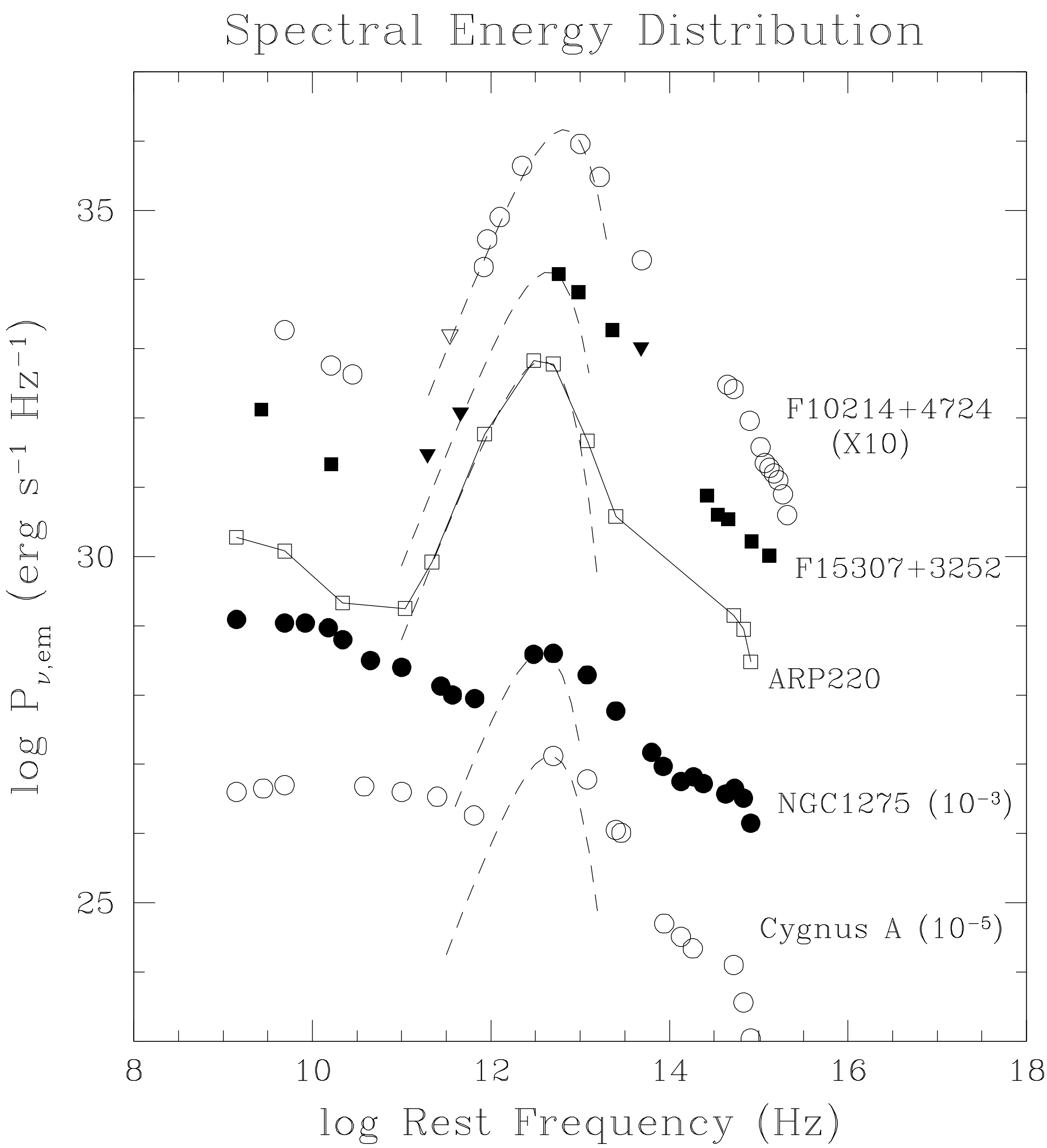

Spectral Energy Distribution
log P$_{\nu,em}$ (erg s^{-1} Hz^{-1})
log Rest Frequency (Hz)
35
30
25
8
10
12
14
16
18
F10214+4724
(X10)
F15307+3252
ARP220
NGC1275 (10^{-3})
Cygnus A (10^{-5})